NASA/CR-20250007038

Blended Wing Body Multi-Discipline Model Development for MBSA&E

Final Report

Matt Johnson and Harsh Patel
Northrop Grumman Corporation, Redondo Beach, CA

August 2025

NASA STI Program . . . in Profile

Since its founding, NASA has been dedicated to the advancement of aeronautics and space science. The NASA scientific and technical information (STI) program plays a key part in helping NASA maintain this important role.

The NASA STI program operates under the auspices of the Agency Chief Information Officer. It collects, organizes, provides for archiving, and disseminates NASA's STI. The NASA STI program provides access to the NTRS Registered and its public interface, the NASA Technical Reports Server, thus providing one of the largest collections of aeronautical and space science STI in the world. Results are published in both non-NASA channels and by NASA in the NASA STI Report Series, which includes the following report types:

- TECHNICAL PUBLICATION.
  Reports of completed research or a major significant phase of research that present the results of NASA programs and include extensive data or theoretical analysis. Includes compilations of significant scientific and technical data and information deemed to be of continuing reference value. NASA counterpart of peer-reviewed formal professional papers but has less stringent limitations on manuscript length and extent of graphic presentations.

- TECHNICAL MEMORANDUM.
  Scientific and technical findings that are preliminary or of specialized interest, e.g., quick release reports, working papers, and bibliographies that contain minimal annotation. Does not contain extensive analysis.

- CONTRACTOR REPORT.
  Scientific and technical findings by NASA-sponsored contractors and grantees.

- CONFERENCE PUBLICATION.
  Collected papers from scientific and technical conferences, symposia, seminars, or other meetings sponsored or cosponsored by NASA.

- SPECIAL PUBLICATION.
  Scientific, technical, or historical information from NASA programs, projects, and missions, often concerned with subjects having substantial public interest.

- TECHNICAL TRANSLATION.
  English-language translations of foreign scientific and technical material pertinent to NASA's mission.

Specialized services also include organizing and publishing research results, distributing specialized research announcements and feeds, providing information desk and personal search support, and enabling data exchange services.

For more information about the NASA STI program, see the following:

- Access the NASA STI program home page at http://www.sti.nasa.gov

NASA/CR-20250007038

Blended Wing Body Multi-Discipline Model Development for MBSA&E

Final Report

Matt Johnson and Harsh Patel
Northrop Grumman Corporation, Redondo Beach, CA

Prepared under Contract 80GRC024CA006

National Aeronautics and
Space Administration

Glenn Research Center
Cleveland, Ohio 44135

August 2025

Level of Review: This material has been technically reviewed by expert reviewer(s).

This report is available in electronic form at https://www.sti.nasa.gov/ and https://ntrs.nasa.gov/

NASA STI Program/Mail Stop 050
NASA Langley Research Center
Hampton, VA 23681-2199

Table of Contents

List of Figures

List of Tables

List of Acronyms

AATT	Advanced Air Transport Technology
ARMD	Aeronautics Research Mission Directorate
BPR	Bypass Ratio
BWB	Blended Wing Body
DOE	Design of Experiments
FEM	Finite Element Model
FLOPS	Flight Optimization System
GASP	General Aviation Synthesis Program
GTOW	Gross Takeoff Weight
HBTF	High Bypass Turbofan
LEAPS	Layered and Extensible Aircraft Performance System
MBSA&E	Model-Based Systems Analysis and Engineering
MDAO	Multi-Disciplinary Analysis and Optimization
MELD	Matching-based Extrapolation of Loads and Displacements
NASA	National Aeronautics and Space Administration
NGAS	Northrop Grumman Aeronautics Systems
OpenVSP	Open Vehicle Sketch Pad
OPR	Overall Pressure Ratio
SFNP	Sustainable Flight National Partnership
SLS	Sea Level Static
SNOPT	Sparse Nonlinear OPTimizer
TACS	Toolkit for the Analysis of Composite Structures
TOFL	Takeoff Field Length
TSFC	Thrust Specific Fuel Consumption
VLM	Vortex Lattice Method
XDSM	eXtended Design Structure Matrix

Executive Summary

Northrop Grumman Aeronautics Systems (NGAS) has developed subsystem models within NASA's Model-Based Systems Analysis and Engineering (MBSA&E) framework that are representative of a concept blended wing body (BWB) commercial transport aircraft. A sizing trade was performed to determine appropriate planform shape to achieve a specified range and cruise condition with a fixed engine. The vehicle sizing trade was carried out using a parametric planform geometry tool that determined the scale, span, sweep, and cabin size based on five design parameters that were varied for the design of experiments. The target characteristics for the BWB sizing was 4000 nautical miles with capacity for carrying 150 passengers.

A representative 3D model was generated in OpenVSP based on the planform selected from the sizing trade. A finite element and vortex lattice model were developed based on the 3D geometry and were subsequently used to perform coupled aero-structural optimization of the vehicle at representative flight conditions. The optimization results show the expected trends with structural thickness sizing and variations in spanload distribution that depend on whether the optimization is considered in a single or multi-discipline coupled fashion.

The models developed under this contract are anticipated to be reusable for future sizing trades on BWB aircraft, as well as for single-discipline and integrated design of static aero-structural interactions. The modularity of the MBSA&E framework allows for higher fidelity trades with custom models to represent individual aircraft disciplines.

1. Introduction

The NASA Aeronautics Research Mission Directorate (ARMD) is currently operating a series of programs and projects through the Sustainable Flight National Partnership (SFNP) to identify, mature and demonstrate technologies deemed enabling for a next-generation, subsonic commercial aircraft. The Advanced Air Transport Technology (AATT) projects is a contributing member of SFNP and is focused on integrating data for technology assessments and determining system-level vehicle performance for these next-generation commercial aircraft. Model-Based Systems Analysis and Engineering (MBSA&E) is an effort within AATT to collate and integrate technology and vehicle data across SFNP. As a part of this effort, Northrop Grumman Aeronautics Systems (NGAS) is under contract to develop engineering component/subsystem models to represent and evaluate a Blended Wing Body (BWB) commercial aircraft configuration using the tools that have previously been developed and integrated into the MBSA&E software framework by NASA. Figure 1 shows how efforts from other SFNP projects are being digitally integrated under the MBSA&E effort.

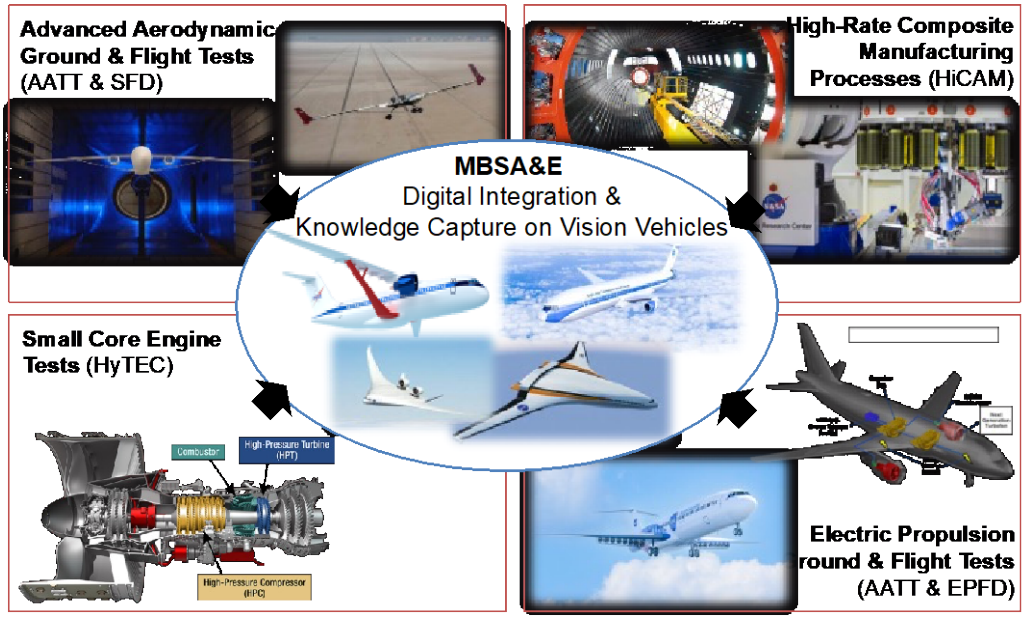

Figure 1: MBSA&E effort to collate and integrate technology and vehicle data across SFNP

NGAS's statement of work under the MBSA&E award was to look at concept-level sizing trades of a blended wing body configuration with NASA's existing toolset that has mostly been applied to conventional tube-and-wing concepts. The other major item was to set up tools for more refined coupled aero-structural trades on a sized BWB vehicle using gradient-based optimization. These optimizations varied aircraft parameters including structural element thickness, wing twist/camber distributions, and angle of attack to minimize drag or structural weight at a given flight condition.

2. Technical Background

The blended wing body is a revolutionary alternative to the tube and-wing configurations that are used in commercial aviation today. Past studies have shown that the blended body configuration can have significantly decreased root bending stresses compared to traditional tube-and-wing configurations, allowing for a lighter wing structure [Ref. 1]. While the BWB concept was first developed decades ago, recent advancements in technology, structural design, materials technology and advanced manufacturing make large-scale production far more achievable.

The reduction in bending loads, combined with the vehicle operating at a significantly lower wing loading, allows for increased structural efficiency. Carefully designed BWB vehicles have the potential to eliminate the empennage surfaces, thereby reducing the wetted area, vehicle drag, and fuel burn [Ref. 2]. For commercial operation, BWB vehicles are also likely to allow faster boarding operations due to the wider, open seating layout therefore decreasing turnaround time during ground operations. Historically, the cabin pressure vessel has been a challenging structural problem since a tube is inherently a lighter pressure vessel to manufacture. Since the internal volume of the vehicle grows faster than the skin area that forms the pressurized cabin, past studies have concluded that BWB vehicles are best used for larger cargo or longer haul commercial passenger flights [Ref. 2].

Northrop Grumman explored the use of a BWB platform to accomplish the mission objectives set forth for a concept design study under NASA N+3 SELECT program in 2010 [Ref. 3], but the range requirement was for shorter-haul flights and a tube-and-wing configuration was determined to be the best path forward for that mission. From 2007-2013 Boeing conducted flight testing of several subscale demonstrator variants, known as X-48. This built on their history of BWB research since the 1990's when McDonnel Douglas (later Boeing) engineers first came up with the BWB concept [Ref. 4]. More recently, the U.S. Air Force has selected aerospace startup JetZero and Northrop Grumman to design, build and fly a full-scale BWB, which aims to demonstrate enhanced capabilities for improved efficiency, endurance and cargo capacity on multi-mission military and commercial platforms. Northrop Grumman will lead mission systems and Scaled Composites, an NG subsidiary, will assist with build, design and test flight of the full-scale air vehicle demonstrator. The work performed by NGAS under the MBSA&E contract is unrelated to any ongoing development efforts or partnerships with JetZero.

Figure 2: Early McDonnell Douglas BWB design, Boeing X48B demonstrator, and JetZero airliner rendering

A traditional structural sizing process seeks to identify the appropriate stiffness of a structural model by applying a fixed set of design loads and resolving strength deficiencies by adding thickness to structural elements or introducing more structural components into the model. Flutter and buckling assessment are later performed on a strength-sized structural model,

which can lead to the identification of additional stiffness requirements that are fed back to an updated structural model.

Prandtl's lifting line theory is the simplest way to understand and calculate lift and it's induced drag for a given wing. For a given wing span, the Prandtl's canonical optimum spanload solution for minimum induced drag is elliptical. In a later 1933 paper, Prandtl determined that there was a spanload solution that gave better system-level drag when an approximation of structural weight was included in the problem [Ref. 5]. Since all aircraft require structural weight to support the air loads, this optimal load distribution (a bell shape, as shown in Figure 3) is the rough shape that conceptual aircraft designers should target. However, there is constant feedback between structural sizing, weight, and optimal load calculation that makes this an inherently multi-disciplinary problem that does not have the simple closed form solution of an ellipse.

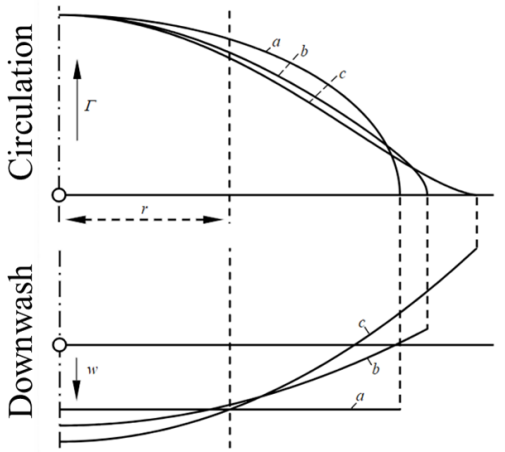

Figure 3: Prandtl's 1933 plots of load distribution and downwash/upwash [Ref. 5]

Early gradient-based optimization research efforts showed the importance of multi-discipline coupling between aerodynamic and structural design. Parallel, uncoupled single-discipline optimizations of these systems did not allow a practitioner to achieve the optimum coupled system. Reuther et al were some of the first to capitalize on advances in aerodynamic shape optimization using adjoint-based design and use them to create aero-structural design frameworks to do coupled sensitivity analysis and optimization [Ref. 6].

In 2016, Bowers revived Prandtl's early theories of bell-shaped lift distributions and made the additional observations that the downwash/upwash field behind a wing with this type of loading would allow for proverse yaw [Ref. 7]. When a roll is induced, the high wing generates a "thrust" from the forward orientation of the tip section resultant force, as shown in Figure 4, resulting in coordinated bank and yaw in the direction of the turn. The consequence of this proverse yaw, later validated with RC flying wing aircraft, is that coordinated flight can be achieved for a flying wing without the need for tail surfaces or wing tip drag devices. The elimination of tails while maintaining acceptable handling qualities, and its connection to the coupled aero-structural sizing problem, makes this a noteworthy effort to pursue in the context of the blended wing body configuration.

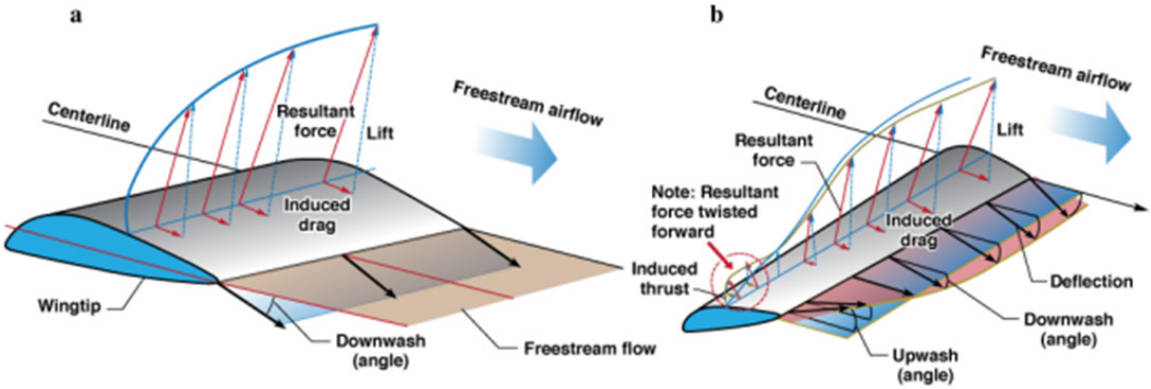

Figure 4: Bowers' 2016 diagrams of tip upwash impact on proverse yaw [Ref. 7]

OpenMDAO is an open-source high-performance computing platform for systems analysis and multidisciplinary optimization, written in Python [Ref. 8]. It enables a user to decompose models, making them easier to build and maintain, while still solving them in a tightly coupled manner with efficient parallel numerical methods. All tools in the MBSA&E framework that are used in this report are built on top of OpenMDAO. MPhys is a package that standardizes high-fidelity multiphysics problems in OpenMDAO. MPhys eases the problem set up, provides straightforward extension to new disciplines, and has a library of OpenMDAO groups for multidisciplinary problems addressed by its standard. The MPhys package is used to handle the couple aerostructural solutions in this report and more information on the problem setup is provided in Section 4.2.

3. Sizing Trades

Considering past studies on the optimal market entry for a blended wing body configuration, the following mission requirements were prescribed for this BWB sizing trade. This mission description is similar to that of the Boeing 757-200, which ended production in 2005 and was a mid-range single-aisle conventional tube and wing commercial transport.

Cruise Altitude (ft)	Cruise Mach	Range (nm)	Passengers	MPG_{GE}	TOFL (ft)
35,000	0.8	4000	>150	>80	<4500

Table 1: Mission requirements for the concept sizing of the BWB

3.1. Aviary Toolset

Aviary is an aircraft analysis, design, and optimization tool that is built on top of OpenMDAO. Aviary includes conceptual-level subsystem models for aerodynamics, propulsion, mass, geometry, and mission analysis as well as the ability to add higher-fidelity or custom user-defined subsystem models. The built-in subsystems draw from legacy tools like FLOPS and GASP that have been used for many years to predict aerodynamics, weights and mission analysis characteristics like range and takeoff distance. The subsystem integration into Aviary, and therefore OpenMDAO, allows for analytic gradient calculation for all these legacy tools and equations.

An XDSM diagram of the subsystem interactions used for the BWB trades is shown in Figure 5. The FLOPS-inspired aero and weights subsystems already had previous applications to BWB configurations [Ref. 9], so the FLOPS subsystem options were primarily utilized instead of the GASP-inspired options.

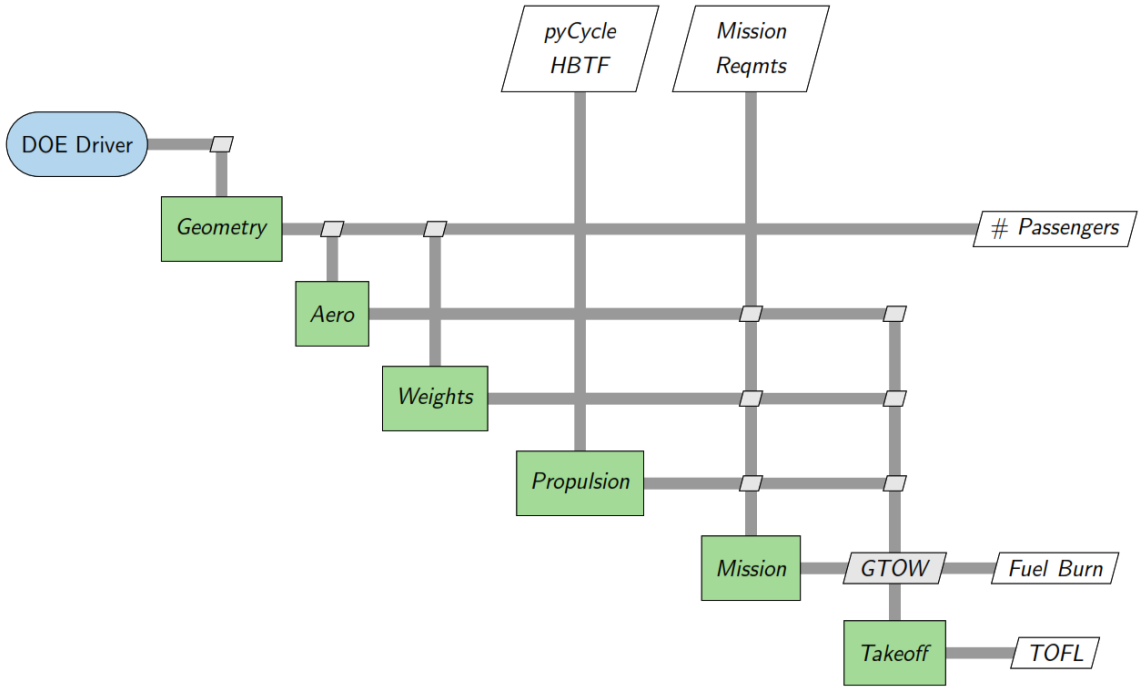

Figure 5: XDSM of Aviary workflow

The primary new subsystem inputs and developments required for building a BWB model within Aviary were: planform geometry definition, propulsion, a mission description, and low speed aero calculations for takeoff.

3.2. Planform Design Variables

A parametric geometry definition of the planform layout was required to run a design of experiments (DoE) without having to manually create an Aviary input file for each point in the design space. There are many ways to define the planform layout with a selected set of dimensions and ratios such that the rest of the common geometric aircraft dimensions become a derived characteristic. Figure 6 gives a summary of the chosen variables and properties for this study that define the "home plate" cabin shape and the outboard wing characteristics. Fall-out characteristics like the chord distribution, which is used by some Aviary subsystems, are measured and fed into those subsystems through the appropriate Aviary input variables.

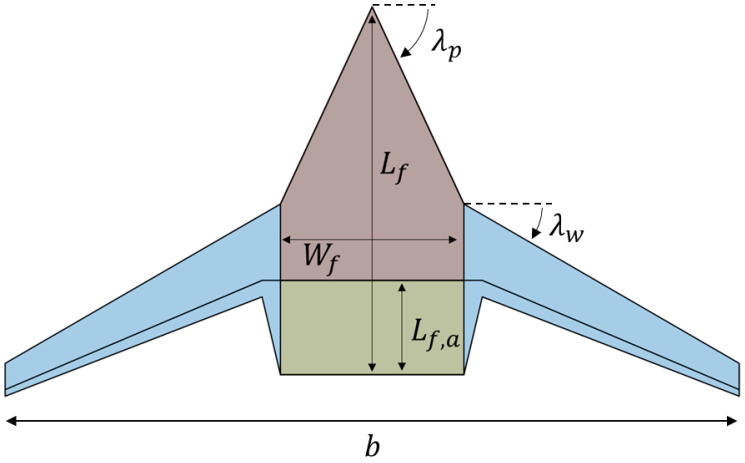

Variables

L_f = total fuselage length
W_f = width of cabin
λ_p = cabin LE sweep
b = wing span
TR = outboard wing taper ratio

Fixed Properties

λ_w = wing LE sweep = 30°
$L_{f,a}$ = aft fuselage length = 18 ft

Figure 6: Planform descriptors

The wing leading edge sweep was held as a fixed property since it would primarily be driven by transonic drag rise and static longitudinal stability requirements, neither of which were considered in sufficient detail within the fidelity of the toolsets used for this sizing trade. The aft fuselage length was frozen at 18 feet since this is where pylon mounted engines would sit on the concept vehicle. Since parametric engine sizes were not considered in this trade, this length was taken to be about 1.5 times the expected engine length (12 ft) to give sufficient space for the inlet duct as well as clearances to the aft bulkhead of the cabin and space between the engine pylon and trailing edge aft closeout. Fixing these properties left the rest of the planform layout fully defined by the fuselage length, cabin width and sweep, as well as the wing span and taper ratio.

A sweep of these design variables gives a wide range of planform options, as shown in Figure 7, with a comparison to the 757-200 and all configurations drawn to scale. Many of these planform shapes, and others that are not shown, are not viable configurations by inspection. The primary reason that these some of these would not reach design closure is small chord lengths. With this chosen set of design variables and ranges, it was also possible to generate planforms with intersecting leading and trailing edges at the wing root. Cases with small or negative chords were eliminated at the geometry-generation step and not run through the rest of the Aviary subsystems.

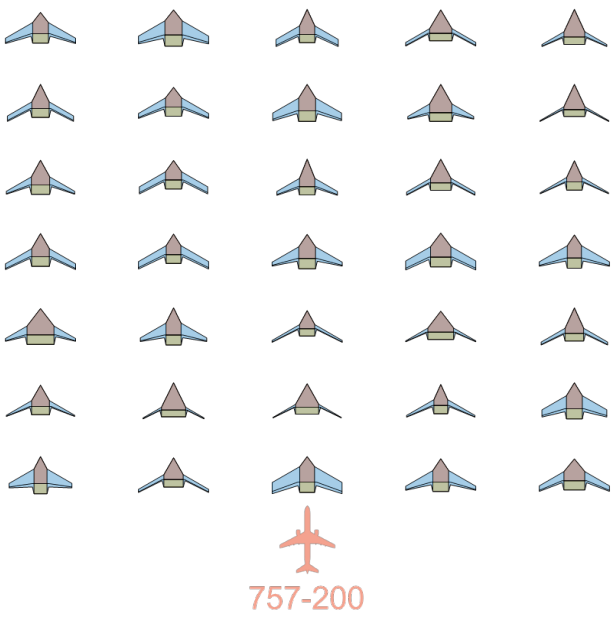

Figure 7: DOE geometry output and down select to useful planforms

3.3. Propulsion Model

The next subsystem that required development for the BWB model was the propulsion component. For this class of aircraft and target design mission, it was expected that a pair of high-bypass turbofans similar to the PW1000G or CFM International LEAP series would meet the requirements and provide currently achievable fuel consumption. Thermodynamic models from OEMs were not readily available for these engines so NGAS set out to put together a representative engine cycle model in pyCycle. A summary of the publicly available data for the target engines is shown in Table 2, along with the resulting characteristics from the pyCycle model.

Engine Name	SLS Thrust (lbf)	Cruise TSFC (lbm/lbf/hr)	Fan Diameter (in)	Engine Weight (lbf)	Cruise BPR	OPR
PW1000G series	15,000 – 35,000	~0.51 (PW1400G)	62 – 88	3,800 – 6,300	9 – 12.5	~42 (PW1431G)
CFM International LEAP	23,000 – 35,000	0.51 – 0.53	70 – 78	6,100 – 8,600	9 – 11	40 (50 @ ToC)
pyCycle HBTF	28,163	0.51	87	-	11	31.7 @ SLS 49.3 @ ToC

Table 2: PyCycle engine properties and comparison to similar engines in production

PyCycle is a thermodynamic cycle modeling library built within the OpenMDAO framework. The modeling library utilizes analytical derivatives within each engine component and these partial derivatives can be used to build total derivative of overall engine performance

with respect to parametric component sizing. This allows for accurate sensitivity calculations that do not suffer from discretization-based issues that would occur with using finite differences to get sensitivities from other thermodynamic cycle modeling tools like NPSS. Parametric studies of the engine parameters were done with an engineer-in-the-loop, but we did not set out to optimize the engines for a specific mission, but rather to approximately match the publicly available data on the Pratt and CFM engines.

The pyCycle engine model operates in two modes depending on whether the goal is to size an engine to a design point or to evaluate the performance of a given engine at an off-design flight condition. In this case, the engine "design" condition refers to takeoff (low speed sea-level) When operating in design mode, a user-specified takeoff engine design thrust target is used to size the internal engine flow path areas given a set of inputs including: fan pressure ratio (FPR), high pressure compressor ratio (HPR), turbine-inlet-temperature (TIT), tubomachinery maps, shaft power extraction, nozzle gross thrust coefficient, and certain station Mach numbers.

In design mode, the engine cycle varies mass flow rate until the target net thrust is achieved, there is no net torque on the shaft, and the fuel-air ratio (FAR) is varied until TIT is hit. This implicit variation of FAR to achieve a target takeoff thrust is achieved with OpenMDAO Balance components. In off-design mode, the engine behaves according to control laws that balances shaft power through spook speed (N_C), targets design nozzle areas by varying bypass ratio, and hits thrust requirements by varying fuel flow. Thrust hook plots in Figure 8 show engine performance at sea level and cruise elevation. These plots show the expected trends of TSFC with thrust and highlight the max SLS net thrust and cruise fuel consumption that are documented in Table 2.

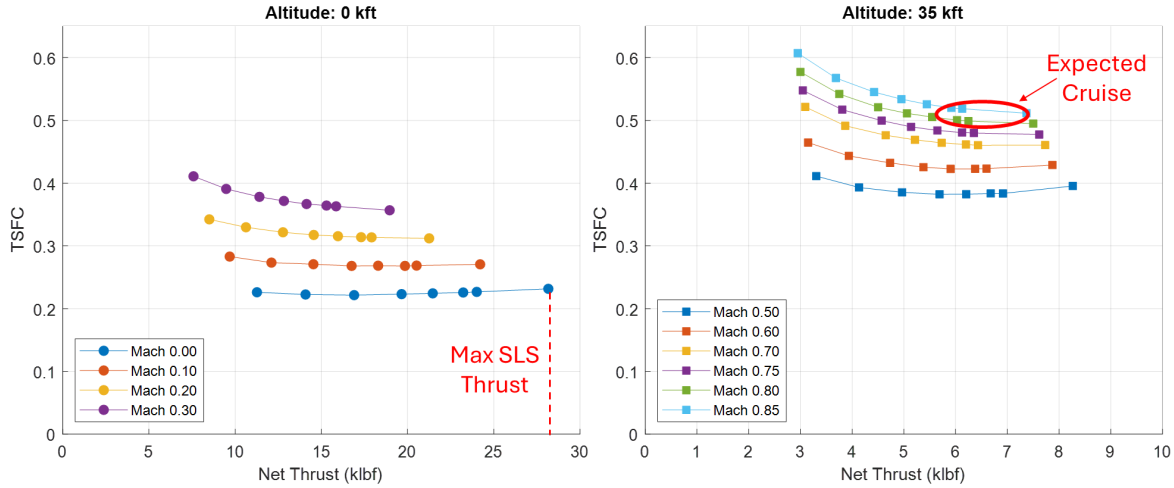

Figure 8: Thrust hook plots of the pyCycle HBTF engine at sea level and 35,000 ft elevation

Five column data was generated by pyCycle across a representative mission envelope. This data was converted to a format that was compatible with Aviary. The mission trajectory optimization uses this five column data to determine required throttle position for a given drag value and therefore get a time history of fuel flow required over a climb-cruise-descent mission.

3.4. Mission Analysis

The mission analysis is a trajectory optimization that takes the weight, aerodynamics, propulsive thrust, prescribed cruise condition, and range to determine the minimum fuel required to complete the mission. The trajectories optimized in this report uses the height-energy

assumptions for equations of motion that is built into Aviary and were originally used in the legacy FLOPS toolset. These equations of motion do not consider the aircraft's flight path angle and treat the aircraft as a point mass without rotational degrees of freedom. The benefits of these simplifying assumptions are robustness and consistency with FLOPS-based subsystems for aerodynamics and weights. The duration in each phase of flight, as well as climb and descent profiles, are optimized to minimize total fuel burn. The mass subsystems built into Aviary does not have any inputs or feedback related to a specific mission and therefore knows nothing about fuel required. The output of the mass subsystem is mission empty weight as opposed to gross takeoff weight (GTOW). The GTOW is calculated by adding the empty weight to the fuel weight required from the mission analysis. This takeoff weight is then passed as an input to the takeoff analysis described in the next section.

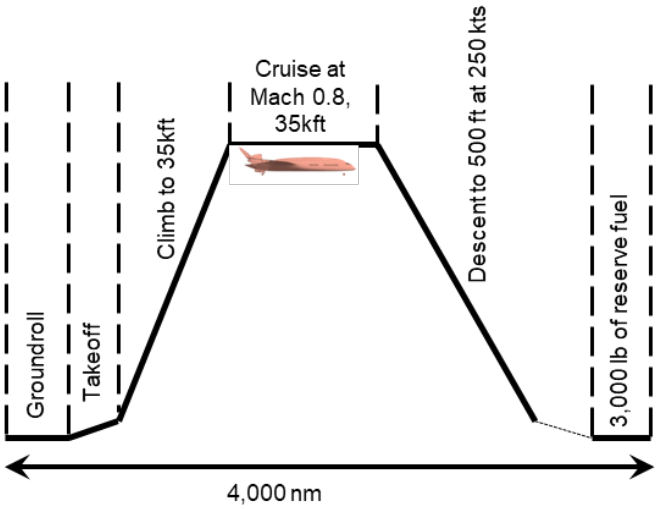

Figure 9: Climb-cruise-descent mission profile

Several candidate planforms were unable to complete the above mission, mostly due to low thrust-to-weight ratios. With large variations in vehicle size and fixed engines, it was expected that some resulting configurations from the DoE would not be able to climb to the cruise condition before running out of excess power. These configurations were either very large, and therefore heavy, or had low aspect ratios that contributed to low aerodynamic Oswald efficiency and therefore high drag.

3.5. Takeoff Analysis

The takeoff analysis used within Aviary relied on the legacy FLOPS-based detailed takeoff. Weight of the vehicle was assumed to be constant at the gross takeoff weight calculated from the mission analysis. All takeoff analysis runs assumes both engines were operative at full throttle. Future cases would require more complexity to determine balanced field length with one engine inoperative. This analysis would require some conceptual assumptions on drag from a windmilling engine, thrust reversal, and a more detailed control surface layout so that trim considerations and their drag impacts can be taken into account.

The initial takeoff roll and climb trajectory to obstacle clearance is shown in Figure 10. V_1, the takeoff decision speed, was not relevant to this study since rejected takeoff and balanced field length were not considered. Distance, velocity and flight path angle were optimized throughout the ground roll, rotation and climb phases to minimize the takeoff distance.

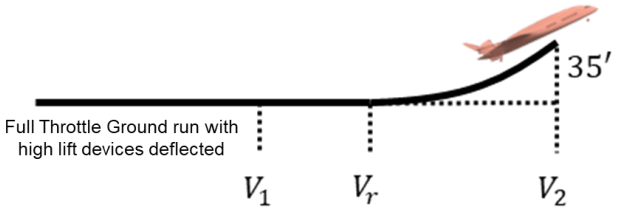

Figure 10: Takeoff diagram showing critical speeds and 35 foot obstacle clearance

In Aviary, the FLOPS-based detailed takeoff analysis does not use the same aerodynamic subsystem analysis that is used for the mission analysis. Instead, arrays for angle of attack and the corresponding lift and drag coefficients are required inputs since they can differ so greatly from the clean-wing aero and are very dependent on the selected high lift control surface layout. A buildup of clean wing lift and drag as well as corresponding high lift control surface increments is shown in Figure 11.

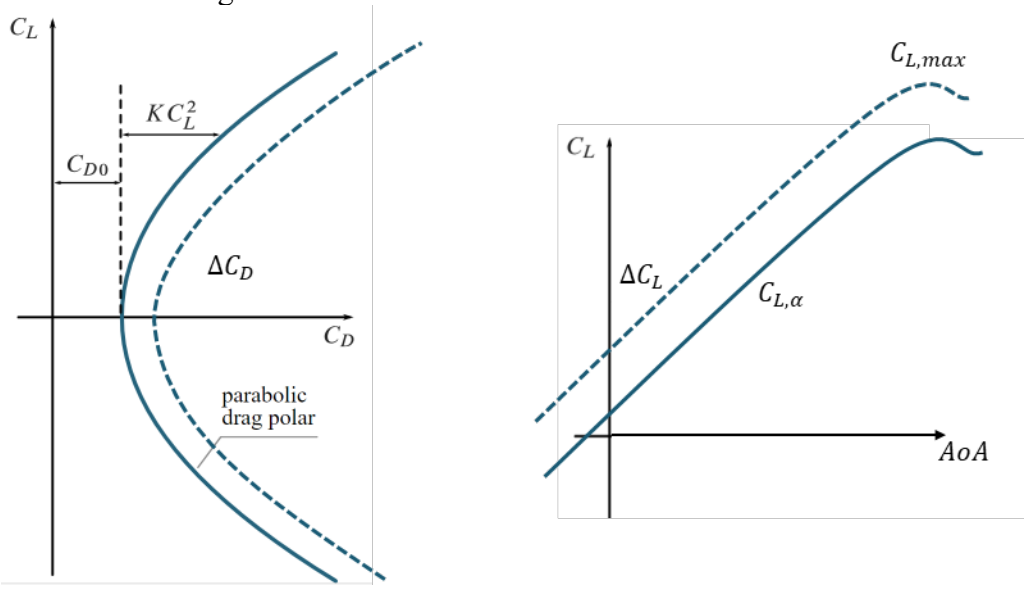

Figure 11: Representative drag polar and lift curve slopes for clean wing and high lift increments

NGAS reused and repurposed aerodynamic calculations from the GASP-based aero subsystem within Aviary to develop these arrays for each candidate configuration, although these components were not used for mission analysis. The legacy GASP components have more detailed empirical aero calculations that include high lift devices. The high-lift control surfaces were assumed to be single-slotted trailing edge flaps with the hinge line at 75% chord, spanning 40% of the outboard wing pane, deflected at 35 degrees.

3.6. Results

After all required subsystems were developed for a BWB sizing trade, a design of experiments was done with the planform design variables as described in Section 3.2. The first sweep of the design space used the design variables ranges shown in Table 3.

Variable	Lower Bound	Upper Bound
Wing Span (ft)	**160**	**200**
Total Fuselage Length (ft)	**70**	**100**
Cabin LE Sweep (degrees)	**50**	**70**
Outboard Taper Ratio	**0.2**	**0.8**
Cabin Width to Span Ratio	**0.2**	**0.4**

Table 3: Initial DoE design variable bounds

400 total geometries were generated, with their reference area and aspect ratio shown in Figure 12. The lower dashed line represents the span lower bound of 160 ft, while the upper line represents the upper bound of 200 ft. As previously described, many of these configurations were not viable because they had very low local chord lengths and there would not be sufficient internal space in the outboard wing to accommodate structural members to support the air loads. These points are labeled as "Failed Geom Checks" and obviously skew toward the high aspect ratio and low wing areas that were considered in the design space. Insufficient thrust-to-weight caused many larger configurations to be unable to reach the cruise condition or require so much fuel to do so that they entered a design weight spiral. These points are denoted by the blue dots in Figure 12. The remaining configurations, 83 out of 400, were considered viable configurations and tend to cluster toward the middle of the geometric design space, as would be expected for this initial wide design space exploration.

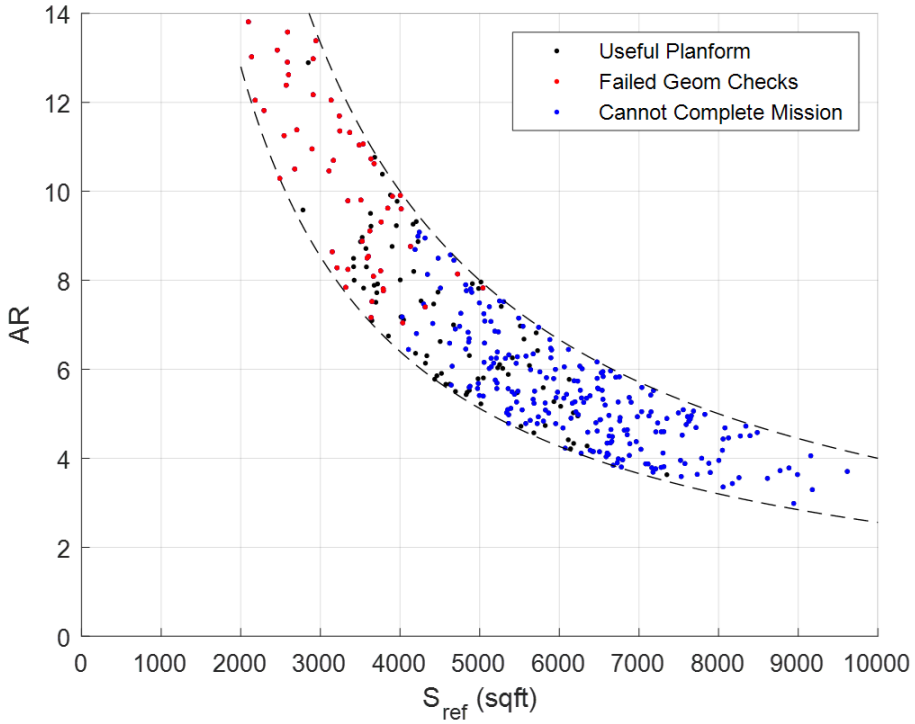

Figure 12: Geometric parameters of candidate planforms colored by pass/fail criteria

After this initial DoE, the resulting fuel efficiency, number of passengers and takeoff field lengths were analyzed. Four promising candidates were selected from this initial set to refine the bounds of the planform design variables. With narrower bounds, almost all configurations in the second set passed the geometry and mission completion checks. Figure 13 shows the numbers of passengers versus passenger miles per gallon (gasoline equivalent) for both the first set (faded) and the second refined set. These points are colored by their gross takeoff weight.

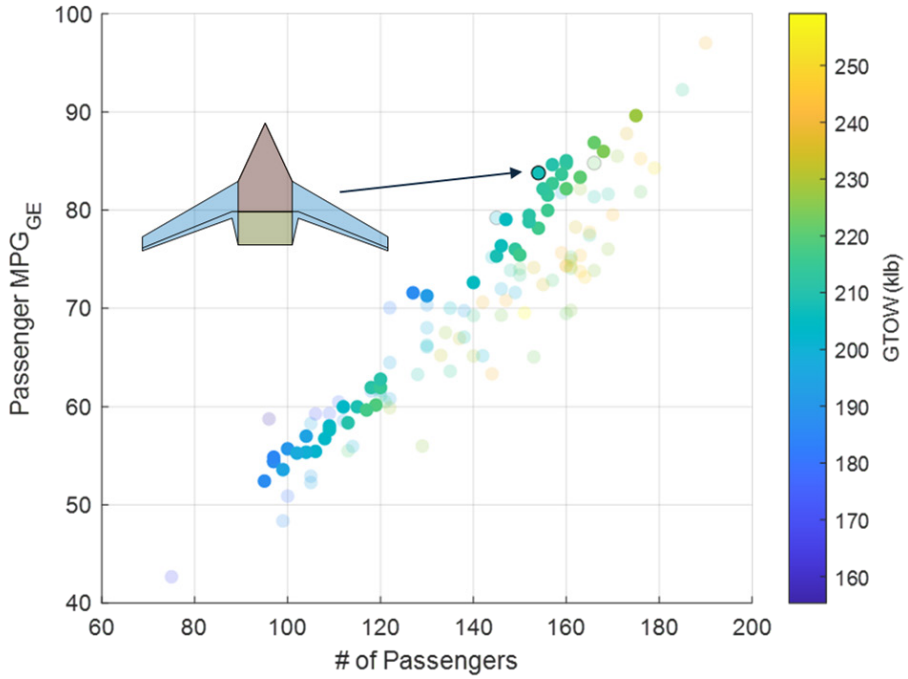

Figure 13: DOE performance results for mission efficiency and passenger count

There are two distinct clusters in the final data set because there is a step change in Aviary's BWB passenger packaging equations when a certain cabin width is reached, and a dual aisle configuration is required. This is due to FAA requirements on number of passengers abreast so that there can be safe evacuation and egress in case of emergency. There is a notable linear relationship between number of passengers and per-passenger fuel efficiency, as expected. The single planform that corresponds to the selected design point and subsequent aero-structural studies is highlighted in both Figure 13 and Figure 14.

Figure 14 shows the output of both the climb-cruise-descent and detailed takeoff performance assessments. The upper left region of this plot is the optimal design space with high fuel efficiency per passenger and low takeoff field lengths. The selected configuration falls along the boundary at the top left of the point clusters and is therefore the best option that satisfies the requirements initially laid out in Table 1.

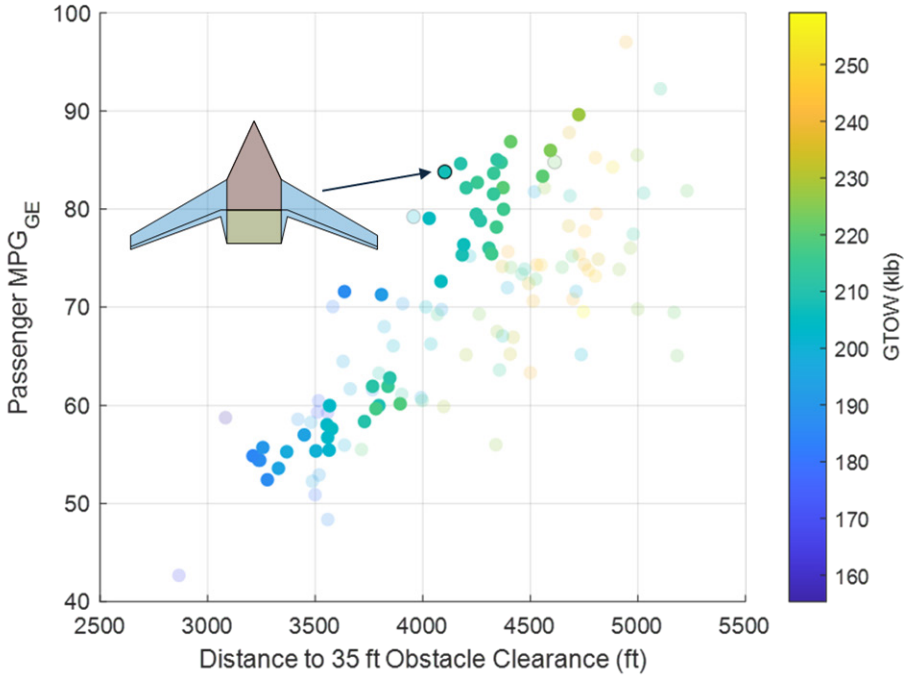

Figure 14: DOE performance results for mission efficiency and all-engines-operating takeoff field length

A summary of the performance, weight, and geometric characteristics for the selected configuration is given in Table 4. Once the planform was fully defined, a 3D OpenVSP model of the BWB was generated.

Passengers	MPG_{GE}	TOFL (ft)	Fuel Weight (lb)	GTOW (lb)	Sref (sqft)	Span (ft)
154	83.8	4102	55,762	207,296	4482	166

Table 4: Configuration and performance outputs for selected configuration

The OpenVSP model shown in Figure 15 allows for both fuel volume verification and FEM development guidance. Aviary's mission analysis capability gives an output for fuel required to complete the mission but knows nothing about the 3D integration of a given fuel tank. It was determined from the OpenVSP model of the selected configuration that a full span skin-to-skin fuel tank between a notional forward and aft spars could hold 87,000 lb of fuel while only 56,000 lb is required to complete the 4,000 nautical mile mission. This leaves sufficient margin for any installation knockdowns that would be required for the tank itself and any other subsystems. If additional fuel space was still available, this configuration could perform extended missions or reduce the spanwise extent of the tank.

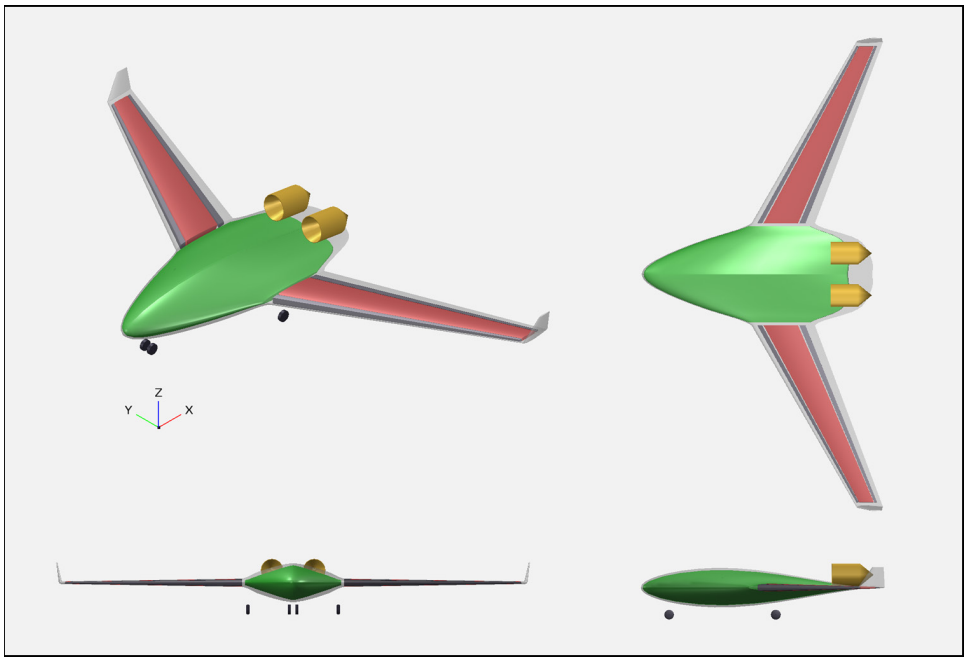

Figure 15: OpenVSP model of BWB aircraft

4. Aero-Structural Optimizations

4.1. FEM Generation

The wing-box finite element model (FEM) of the BWB, which is shown in Figure 11, was created using PATRAN. The FEM output of PATRAN is a NASTRAN bulk data file (BDF) for SOL 101 linear statics analysis, however the same file can be imported into TACS for information about the geometry, loads, boundary conditions, materials, etc. Two uniform load cases were initially defined over the upper surface: one for 1 psi up-bending and another for -0.33 psi down-bending. The FEM also includes discrete loads from the engine mounts and the landing gears, which are modeled by concentrated masses (CONM2). The lower skin of the FEM has three rectangular cutouts defined by the keel and spar spacings, modeling the main and nose landing gear bay door cutouts on the BWB.

The BWB wing-box consists of structural components including conventional spars, ribs, and skins to support the aerodynamic loads encountered during flight. The spars are longitudinal beams that run spanwise along the wings and provide structural support and strength. These components carry the majority of the aerodynamic forces and moments generated during flight. Ribs positioned perpendicular to spars along the wing span, shape the wing profile and counteract twist and torsion. They evenly distribute pressure and shear forces across the wing's chord, enhancing structural strength. The skin, the outermost layer, forms the aerodynamic surface exposed to airflow and encases the internal wing-box structure, providing streamlined shape and resistance to bending and torsion.

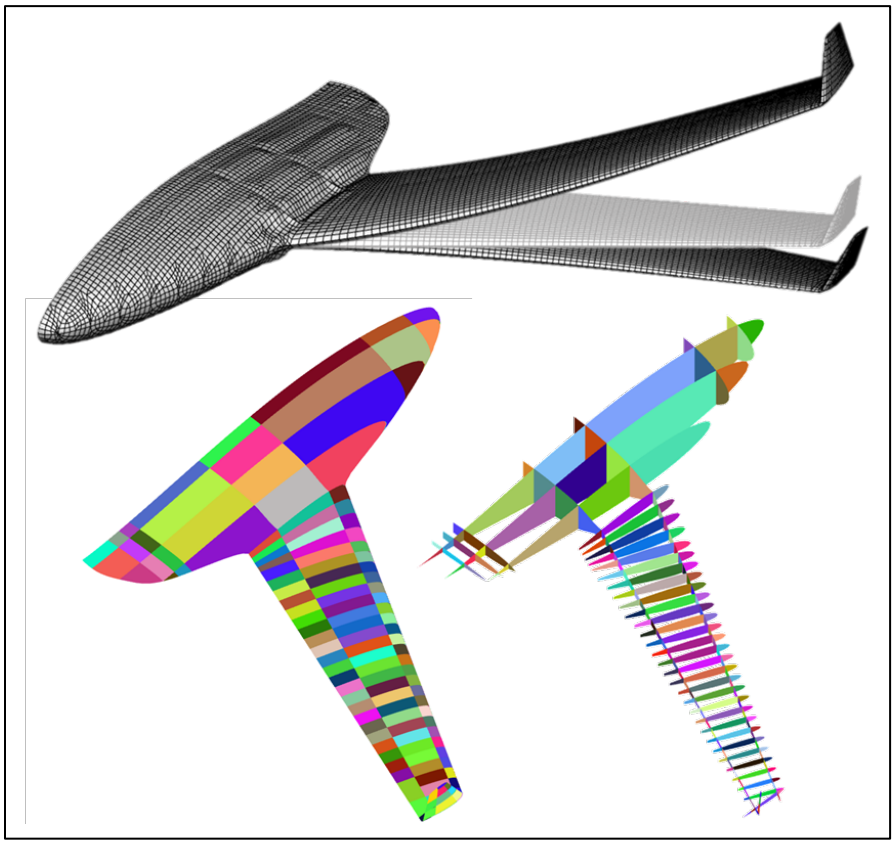

Figure 16: BWB FEM mesh and structural component patches. Each patch has independent thicknesses.

In the FEM, thickness can be parameterized and optimized using shell element design variables. Shell elements, defined using PSHELL property cards for single-material shells, provide precise control over local thickness. The BWB FEM comprises standard four-node quadrilateral shell elements (CQUAD4) and three-node triangular shell elements (CTRIA3). The thickness of these elements directly influences both the stiffness and mass of the aircraft structure; a thicker shell element increases bending stiffness and load-carrying capacity but also adds more weight to the structure. The FEM comprises 13,779 nodes and 15,616 shell elements, and the model of the aircraft structure is assumed to be aluminum for the analysis and optimization cases that were completed. The material density of aluminum is set as 2,796 kg/m3, with a modulus of elasticity of 71.02 GPa and a shear modulus of 26.70 GPa.

4.2. MPhys Toolset

As part of the OpenMDAO ecosystem, MPhys was introduced as a modular multiphysics simulation package that standardizes multi-fidelity analysis and design optimization. Built on top of OpenMDAO, MPhys provides unified interfaces for a variety of multiphysics solvers, enabling seamless management of inter-solver couplings within the framework. MPhys interfaces ensure standardization of outputs, such as states, residuals, and functionals, to OpenMDAO, facilitating data transfer between each model and enabling the solution of coupled analysis and optimization problems.

We leverage MPhys interfaces for coupling in an OpenMDAO framework to carry out aerodynamic, structural, and aero-structural optimizations, utilizing a gradient-based optimizer. In this section, we describe various solver components integrated in this framework. OpenAeroStruct is an open-source multidisciplinary framework built on OpenMDAO, combining low-fidelity aerodynamics and simple finite-element structural analysis for coupled aero-structural optimizations, however we only use its aerodynamic modeling capabilities to compute the flow solution and aerodynamic loads in this work. For aerodynamic modeling, OpenAeroStruct uses a vortex lattice method (VLM) to model lifting surfaces such as aircraft wings and tails. The VLM is limited to simulating inviscid, incompressible flows over the lifting surfaces, but it provides rapid aerodynamic estimates for lift and drag, as well as load distribution, in conceptual aircraft design.

The Toolkit for the Analysis of Composite Structures (TACS) is a parallelized finite-element code for analysis and gradient-based design of advanced metallic and composite structures. TACS is responsible for computing static displacements in the coupled aero-structural analysis and is capable of modeling and analyzing both linear and nonlinear structural behavior, encompassing static, dynamic, as well as thermal analyses. These features enable accurate simulation of diverse loading conditions and environmental factors. Equipped with state-of-the-art solver algorithms and numerical methods, TACS efficiently tackles complex structural problems with its extensive library of finite elements, material models, and boundary conditions.

The coupling of aerodynamics and structures involves a load and displacement scheme, with matching-based extrapolation for loads and displacements (MELD) facilitating loads and displacements transfers between OpenAeroStruct and TACS at each aero-structural iteration. MELD establishes connections between individual aerodynamic surface nodes and groups of structural nodes. The displacement of each aerodynamic node is determined by aggregating the displacements and rotations of its associated structural nodes, computed via a least-squares fit. This method relies solely on node positions and displacements and is independent of mesh

connectivity.

We utilized pyOptSparse, a specialized optimization framework tailored for constrained nonlinear optimization of large sparse problems. In this study, we employ Sparse Nonlinear OPTimizer (SNOPT) for all optimization tasks presented. SNOPT is a sequential quadratic programming (SQP)-based optimizer explicitly designed for large-scale nonlinear constrained problems. SNOPT offers a comprehensive suite of customizable options, facilitating fine-tuning of the optimization algorithm's performance.

To solve the coupled aero-structural governing equations, we use the nonlinear block Gauss-Seidel (NLBGS) algorithm. In the NLBGS approach, as shown in the eXtended Design Structure Matrix (XDSM) diagram in Figure 17, the aero-structural state variables are initialized with q_0 and u_0, while the MELD transfer scheme starts with zero structural displacements u_s. The VLM flow solver in OpenAeroStruct is then used for the initial aerodynamic analysis to calculate the aerodynamic forces f_a acting on the OML. These aerodynamic forces are converted to nodal structural forces f_s using the MELD transfer scheme. Subsequently, these forces are transferred to TACS for structural analysis, providing updated structural displacements u_s. These displacements are then transmitted back to the VLM solver in OpenAeroStruct using the MELD displacement transfer. Subsequently, the fluid mesh is deformed based on the aerodynamic surface displacements u_a, leading to an updated flow solution. This iterative process continues until the desired convergence criterion is achieved, yielding the converged aero-structural state variables q^* and u^*.

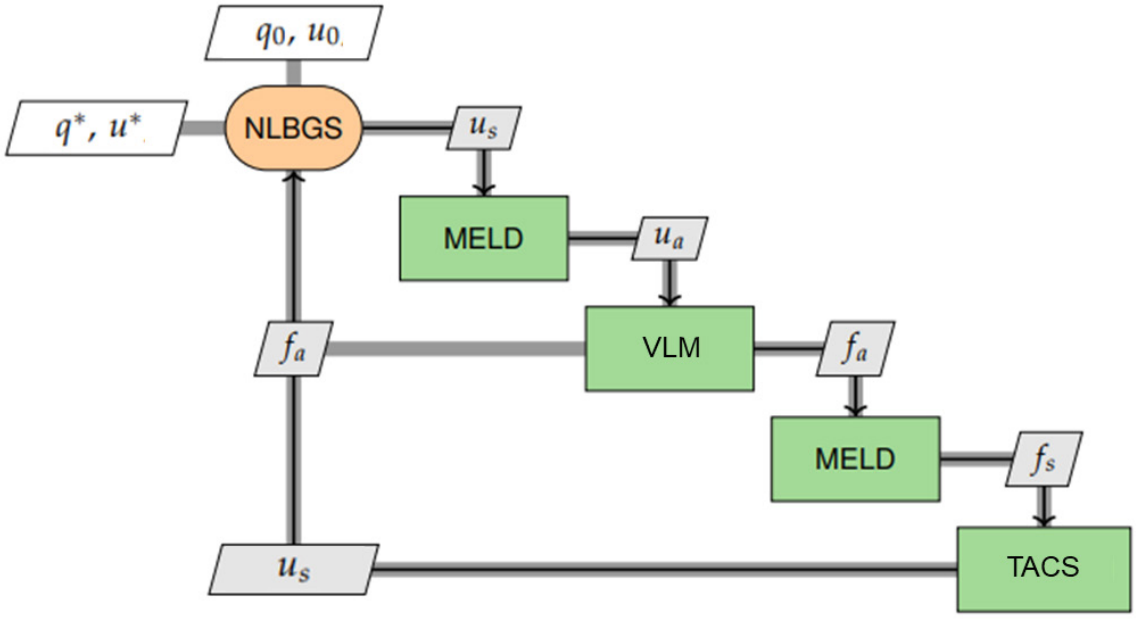

Figure 17: XDSM diagram of the nonlinear block Gauss-Seidel (NLBGS) aero-structural solution

4.3. Aero Optimization Results

Aerodynamic shape optimization of the BWB was performed at the cruise condition in inviscid flow with different wing design variable combinations. The BWB OpenVSP model was used to create a VLM panel mesh in OpenAeroStruct and is shown in Figure 18.

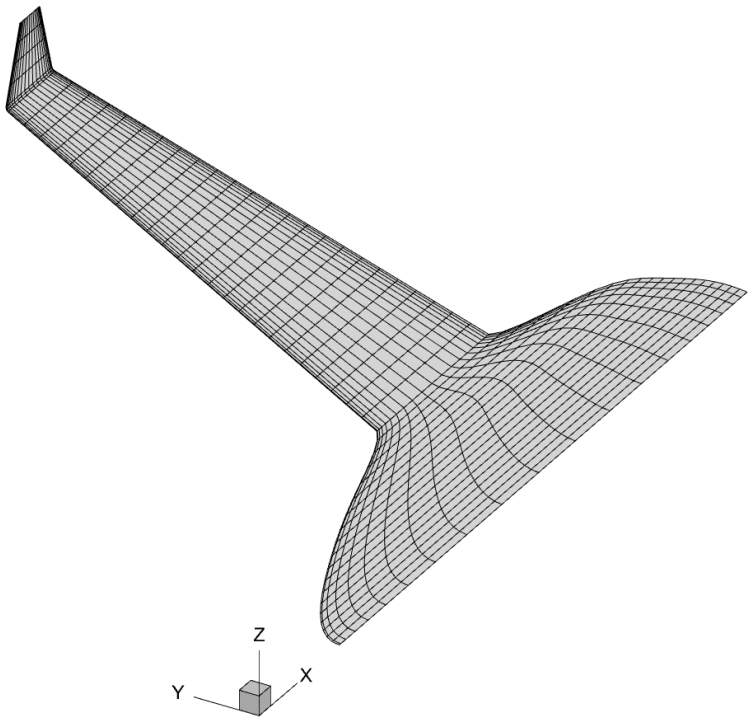

Figure 18*:* Aero VLM mesh.

Solutions to the VLM at a given flight condition yield pressure differences between the upper and lower surfaces at each vortex panel. These pressure differences are integrated over all panels to yield the aerodynamic forces, moments and spanwise load distributions. A plot of the VLM solutions before and after a drag optimization that controls camber and twist is show in Figure 19.

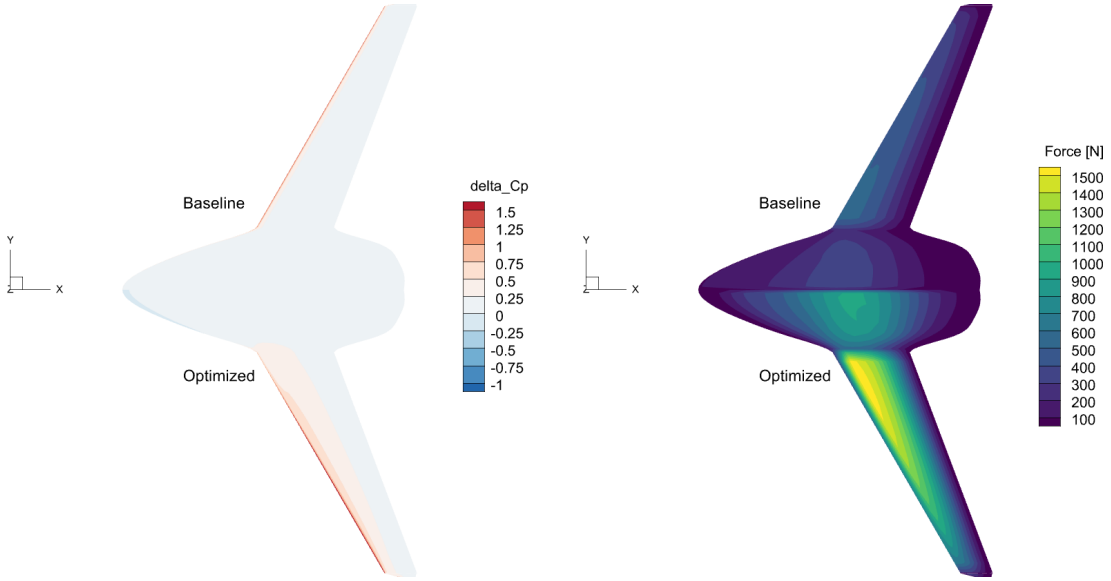

Figure 19*: C_p and force contours for aero-only VLM optimization for target C_L of 0.2*

The goal of this optimization was to minimize total drag by adjusting the aircraft shape through changes in camber and twist, which are parameterized through OpenVSP with airfoil control stations. Airfoil thickness parameter have no impact on the VLM solution and are not used as design variables. The objective is to redesign the wing shape to minimize drag coefficient while maintaining a constant lift coefficient that corresponds to level flight at cruise. The primary mechanism for reducing drag at this condition, with a fixed planform shape, is to reduce the induced drag by controlling the spanwise load distribution. The canonical lift distribution shape for minimum drag from lifting line theory is elliptical. The result of three optimizations is shown in Figure 20 where the number and type of design variables were varied. Camber and twist were controlled at several spanwise locations and when either type of aerodynamic control were given to the optimizer, the optimized drag came to a similar results. However, when both camber and twist were given and there were more degrees of freedom, the optimizer was able to achieve a slightly better result and came very close to a purely elliptical lift distribution.

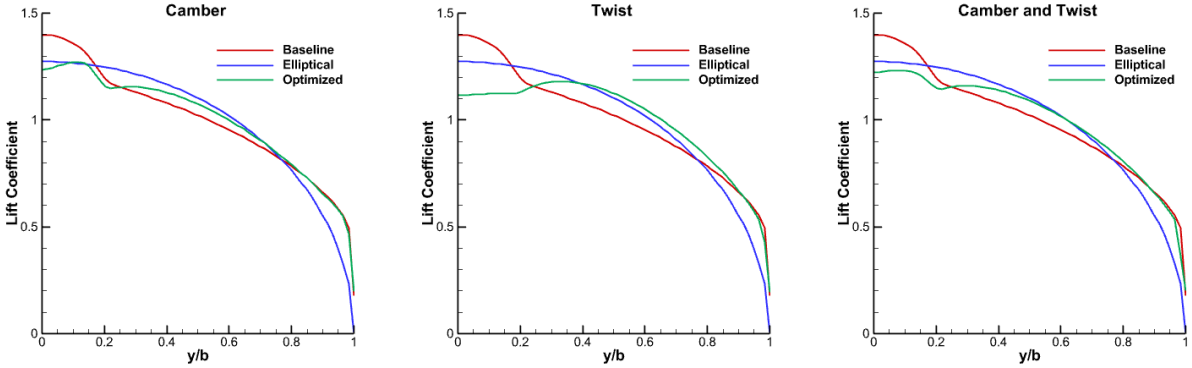

Figure 20: Spanload distributions from aero-only VLM optimization for a target C_L of 0.2.

4.4. Structural Optimization Results

Next, a structural thickness optimization was performed on the BWB FEM, using TACS to perform linear statics analysis. One case was run with fixed uniform loads applied to the upper surface and another using loads transferred from VLM results to get a more realistic chordwise and spanwise load distribution representative of flight.

The goal was to perform a structural sizing analysis to assess the impact of aerodynamic loads on required material thickness and structural mass. The objective function is the aircraft structure's weight, with stress constraints applied to all quadrilateral and triangular shell elements, as well as thickness design variable bounds. The workflow includes an option for stress constraint aggregation using the Kreisselmeier–Steinhauser (KS) function, which conservatively estimates the maximum failure, ensuring a conservative design.

The initial condition for the optimization was a uniform structural thickness of $1/8^{th}$ inch on all surfaces. The resulting optimal thickness of the structural elements is shown in Figure 21 for the case with fixed VLM-based aero loads. Almost all element thicknesses are reduced to the minimum bound except at the wing root junction on the spars and skins. This is expected as this is the location where the maximum stress is located and adding thickness in other locations simply adds weight and penalizes the objective function. All stress constraints were satisfied for this optimizer result with the stress level equal to the failure criteria in the region of the wing root.

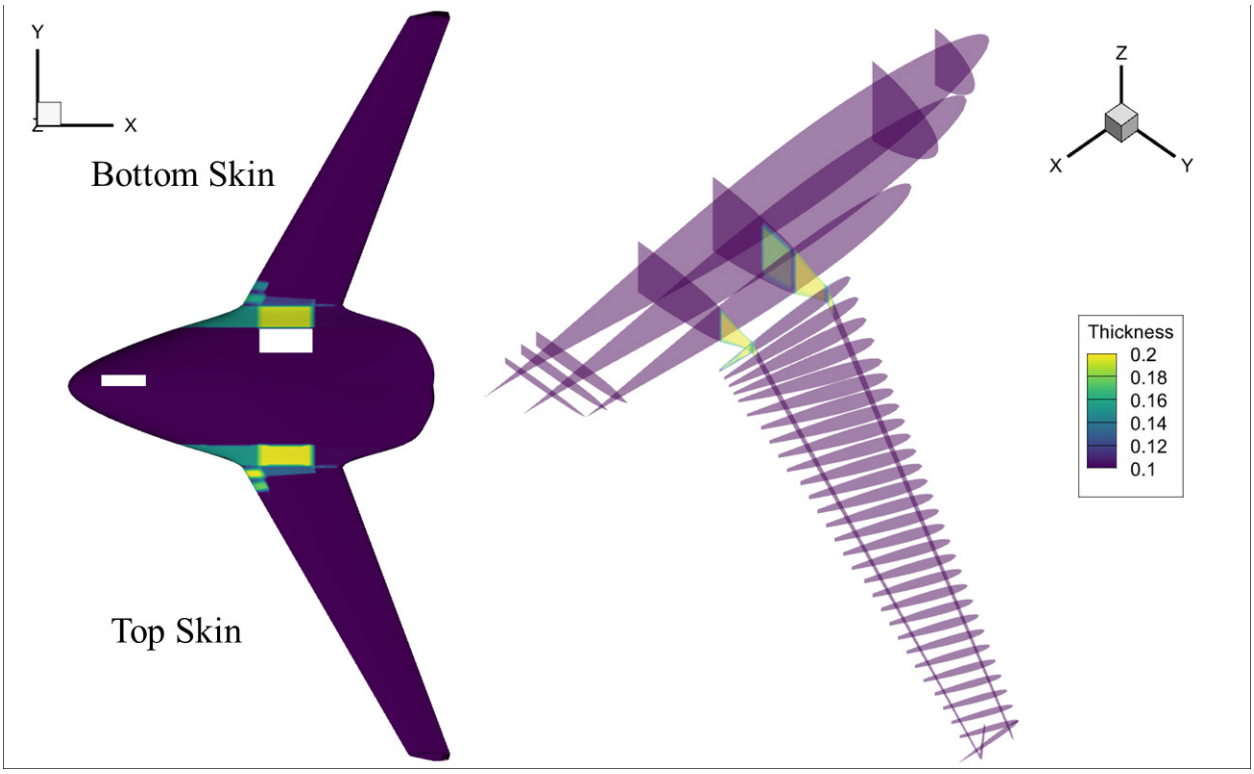

Figure 21: Optimized FEM thickness distribution for structures-only optimization

The white boxes shown on the bottom skin are the representative cutouts for forward centerline and aft main landing gear bays. These sections of the skin are doors and cannot distribute loads to adjacent skin sections and are therefore not included in the FEM.

4.5. Coupled Aero-Structural Optimization Results

Finally, a simultaneous optimization of aerodynamic shape and structural sizing was performed for the BWB. The two objectives tested were to minimize either the aircraft's weight or the total drag coefficient. The design variables encompass the aero parameters of camber and twist, as in Section 4.3, as well as the structural shell thicknesses parameters that were used in Section 4.4. We also experimented with introducing an additional angle of attack design variable for two of the drag minimization optimizations.

For all cases, the lift coefficient was constrained to a specified target to ensure sufficient lift for steady level flight. A structural KS stress aggregation function was also applied to all problems, such that it would not exceed the design stress limit. Thickness bounds were set from 0.1 inches to 0.3 inches. Attempts were made to run with wider design variable bounds but large optimizer step sizes would sometimes cause poor convergence and/or unreasonable deflections in the structural model that made the coupled NLBGS aero-structural solver fail and the optimizer would terminate. A summary of potential future solutions is provided in Section 5.

The optimal thickness of the structural elements is shown in Figure 22 for a case that targeted minimum drag. Thicker structural elements are more widely distributed in this case than the structures-only case since the objective is to minimize total drag instead of only focusing on the weight of the structure.

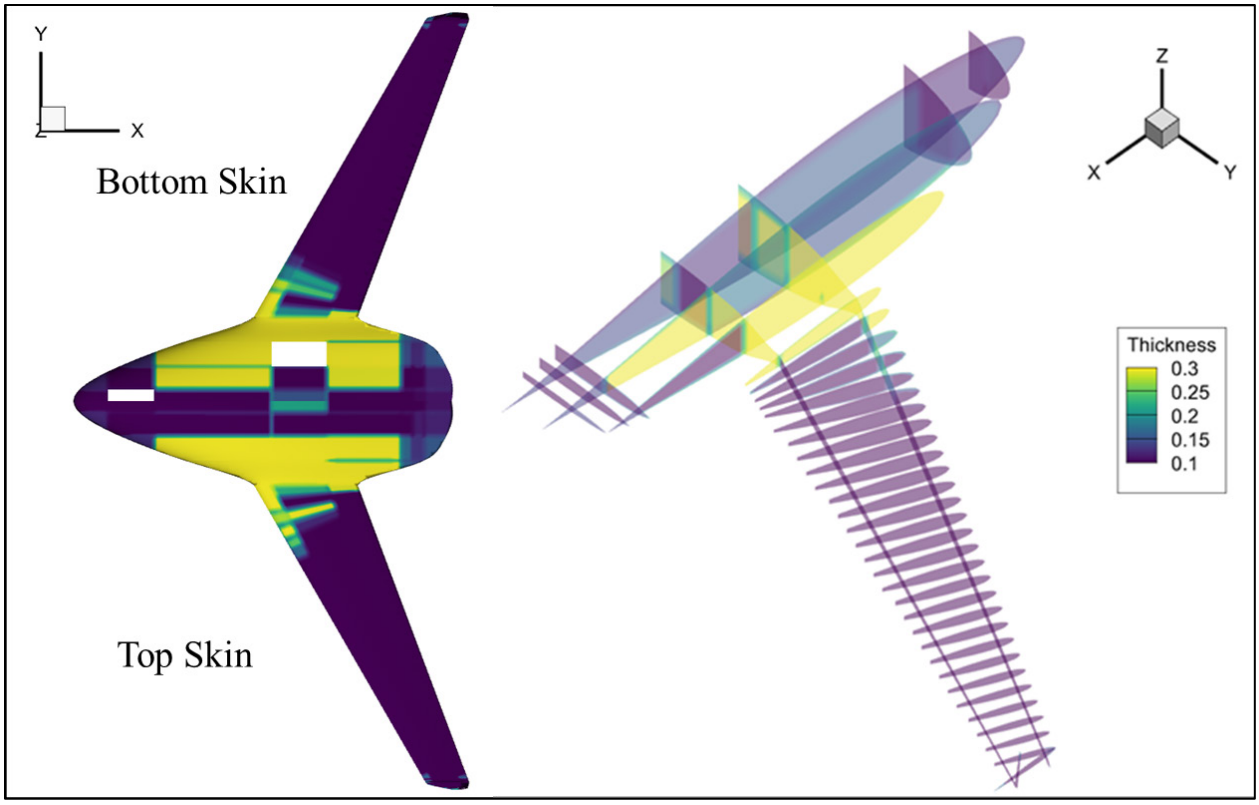

Figure 22: Optimized FEM thickness distribution for coupled aero-structures optimization on drag

The baseline loading case and uniform structural thickness distribution resulted in stress constraint violations as shown in Figure 23 where the failure contour is greater than one. The stress is concentrated on the forward and aft spars at the wing root junction, as well as the adjacent skin panels. This pattern of stress remains in the optimized case but the stress constraints have dropped below the failure criteria at their peak locations.

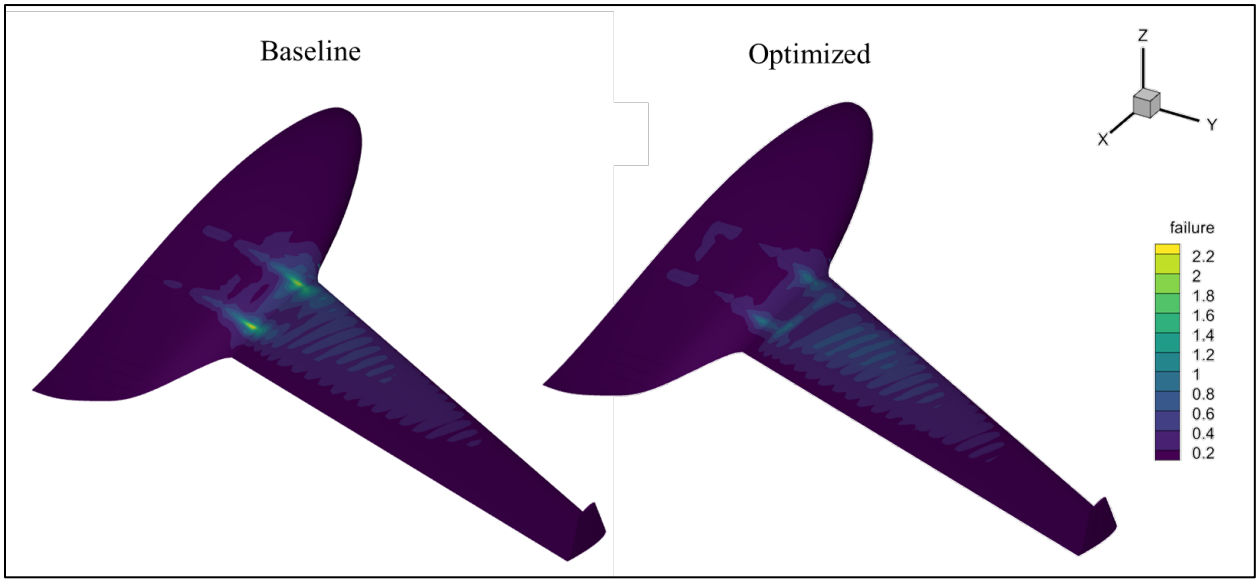

Figure 23: Contours of normalized stress concentration on the skin of the baseline and optimized BWB

The red and blue curves show a similar pattern to the analytically calculated optimal load distributions in Figure 3. The uncoupled aerodynamic-only optimizations trends toward and elliptical normalized load distribution from the baseline condition. However, the coupled aero-structural case leads to a bell shape where the outboard section of the wind is unloaded in order to satisfy stress constraint requirements at the wing root. The difference between these solutions and the analytically derived Prandtl solutions is that we are sizing the actual structural elements in the FEM instead of relying on the assumption that the spar weight at each location is simply proportional to the bending moment and therefore the "moment of inertia" of the lift distribution is fixed, as Prandtl described it ([Ref. 5]).

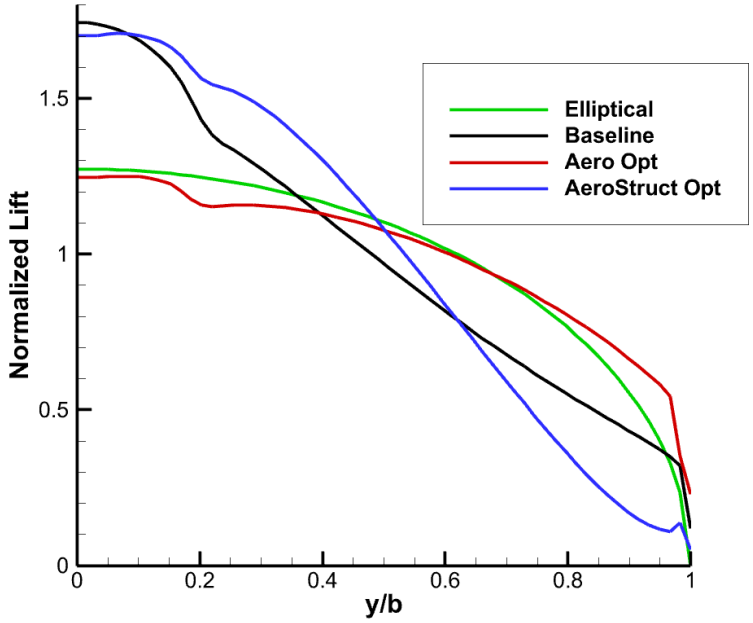

Figure 24: Resulting spanwise load distribution for the aero-alone and aero-structural optimizations

The optimizer convergence history for the coupled aero-structural case is summarized in Figure 24. The feasibility and optimality criteria show good convergence, though they do not both reach the target value of 1E-6 over the 50 allowable major iterations. The initial spike in the objective function is an effort to get feasible on the initial constraints at the cost of the objective function, but after the initial increase, there is a monotonic decrease to the final drag value. More details on optimizer convergence can be found in Appendix A.

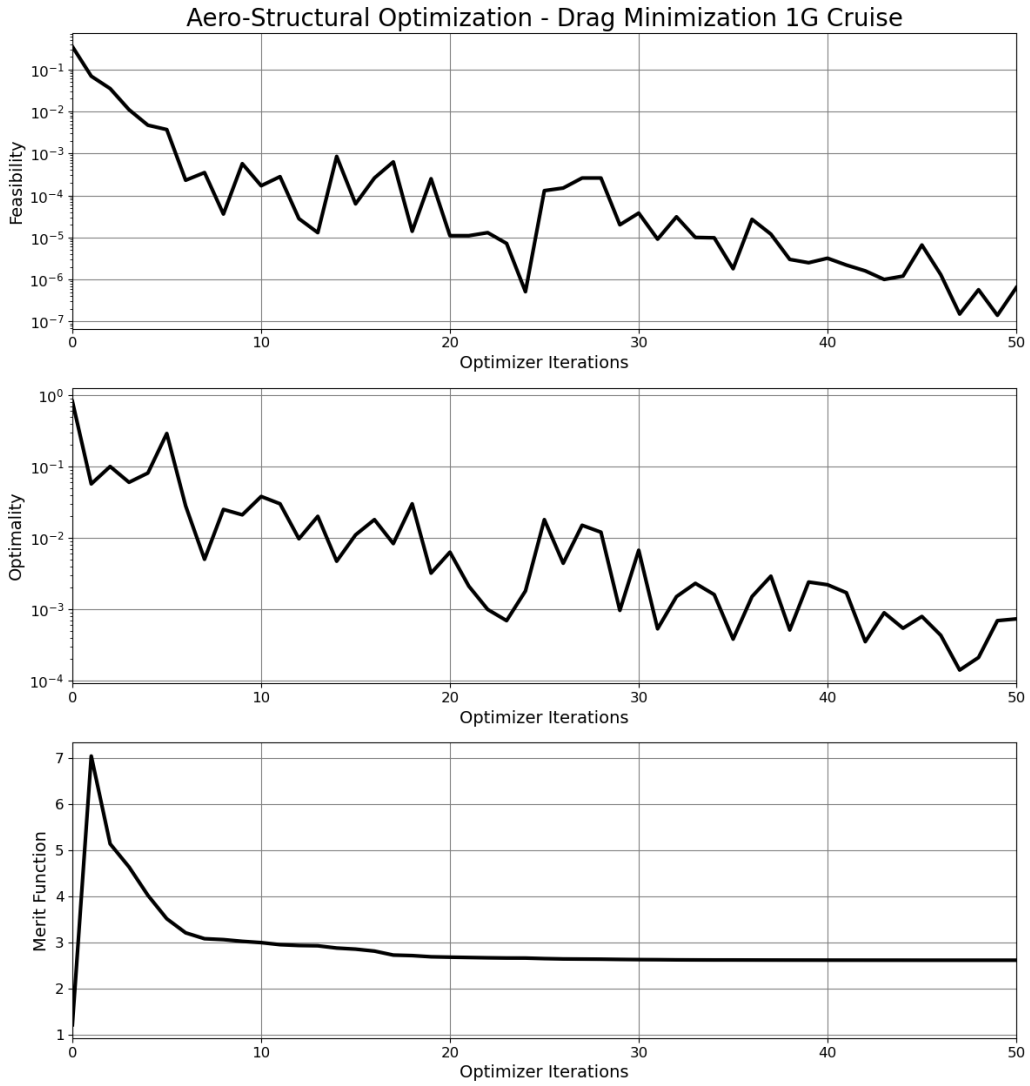

Figure 25: Convergence history of optimizer for coupled aero-structural case

5. Summary and Recommendations

Under this contract, NGAS has created representative Aviary subsystem models that allow sizing trades of a blended wing body commercial transport configuration. A parametric planform geometry tool allowed large-scale design of experiments to evaluate mission-level fuel efficiency and detailed takeoff assessments. Using the existing MBSA&E toolsets and their associated fidelities, a configuration was selected from the DoE that met the conceptual-level sizing design requirements. This 2D layout was converted to a 3D OpenVSP model for fuel volume and integration assessments. This model was also used to generate a baseline finite element model that captures a notional internal structural layout. This FEM was then used in conjunction with vortex-lattice aero modelling to run a series of optimizations building to a coupled aero-structural optimization problem that focuses on either reducing structural weight or aerodynamic drag. This work advances capabilities in rapidly trading BWB configurations with options to increase fidelity on an individual subsystem level and pursue the SFNP key technology objective of exploring advanced and novel aero configurations.

In some of the coupled aero-structural optimization, drastic differences in shell thickness between adjacent elements were observed. These large variations in the structural thickness led to numerical instabilities in the structural solver, causing the optimization to fail. Future work could implement adjacency constraints for the structural thickness design variables, which will ensure relatively smooth transitions between adjacent thickness values. The optimization process will become more robust and should improve optimizer's convergence behavior.

In this work, multiple flight conditions were evaluated for the BWB (i.e. 1G cruise and 2.5G pull-up maneuver), but they were analyzed independently. Future work should focus on extending the current aero-structural framework to incorporate multi-point optimizations, enabling the simultaneous consideration of multiple flight conditions and aircraft maneuvers. Relying solely on a single flight condition to define an aircraft design is inadequate, as slight deviations from that point can lead to significant performance detriments, increased weight, and unnecessary margins. Introducing multiple competing requirements allows for design compromises while also ensuring the development of a robust wing design. Therefore, advanced design efforts must incorporate a fully-aeroelastic conceptual model and shape optimization methodology capable of accounting for aeroelastic effects at a variety of flight conditions.

All optimization problems discussed in this work pertain to linear statics strength-sizing problems, but other structural modeling considerations are equally important, for example buckling and flutter. Buckling is a critical failure mode for thin-walled aircraft structures subject to significant compressive loads. Linear statics focuses on determining overall structural deformation and stresses under some applied load assuming there is no instability, whereas buckling analysis assesses the critical load at which a structure becomes unstable and experiences sudden large deformations. Incorporating buckling analysis would enable more comprehensive and accurate assessment of structural stability under aero-structural loads, providing greater insight about aerodynamic and structural performance for a conceptual BWB design.

A unique benefit for bell-shaped lift distributions on blended wing bodies is the possibility of achieving proverse yaw due to the upwash experienced near the wing tip. Achieving proverse yaw, where a vehicle turns into a roll maneuver naturally, will mitigate some of the control difficulties related to flying a BWB with no tail surfaces. Further studies into how a coupled aero-structural optimization could incorporate handling qualities and controllability

constraints would likely yield a much more mature vehicle concept.

The modularity of Aviary, and the OpenMDAO framework it is built on, allows for external tools to be used in the evaluation of core mission analysis subsystems. Since there is a relatively high uncertainty in weight estimates for a full-scale commercial transport blended wing body, it may be useful to use a higher fidelity structural sizing tool in an Aviary sizing trade. With the appropriate constraints and sizing criteria, i.e., including buckling and cabin pressure vessel sizing, a higher fidelity structural sizer will likely produce a more accurate structural weight estimate than Aviary's empirical estimation methods, albeit at a higher computational cost. A more accurate representation of the structural weight variation with planform shape could drive the aircraft layout to a different region in the design space.

Appendix A: Optimization Convergence Summaries

A summary table of all optimization problem statements and final results are included below. Eleven total optimizations were run to see how changes to the design variables, objective, constraints, and coupling impacted the final solution for the aerodynamic and structural solutions. The software models, as well as all input and output files, are included in the contract deliverables as well for future reference.

Aerodynamics								
	Name	**Baseline**	**Optimized**	**Target**	**Lower**	**Upper**	**Scaler**	**Units**
Case 1 - camber, cruise, VLM loads								
Objective	drag	0.002067	0.005708				1.00E+03	
Constraints	lift	0.206491	0.35	0.35			1.00E+01	
Design Variables	camber	0			0	0.05	1.00E+02	
Case 2 - twist, cruise, VLM loads								
Objective	drag	0.002068	0.005662				1.00E+02	
Constraints	lift	0.206499	0.35	0.35			1.00E+00	
Design Variables	twist	0			-10	10	1.00E-02	deg
Case 3 - camber and twist, cruise, VLM loads								
Objective	drag	0.002067	0.005608				1.00E+03	
Constraints	lift	0.206491	0.35	0.35			1.00E+01	
Design Variables	camber	0			0	0.05	1.00E+02	
	twist	0			-10	10	1.00E-01	deg
Structures								
	Name	**Baseline**	**Optimized**	**Target**	**Lower**	**Upper**	**Scaler**	**Units**
Case 4 - uniform static loads								
Objective	mass	9012.28	4963.459				1.00E-03	kg
Constraints	stress	0.640362	1		0	1	1.00E+00	
Design Variables	thickness	0.003175	0.00105		0.001	0.005	1.00E+03	m
Case 5 - VLM loads								
Objective	mass	9012.28	5389.719				1.00E-03	kg
Constraints	stress	2.21312	1		0	1	1.00E+00	
Design Variables	thickness	0.003175	0.00115		0.001	0.005	1.00E+03	m
Aero-Structural								
	Name	**Baseline**	**Optimized**	**Target**	**Lower**	**Upper**	**Scaler**	**Units**
Case 6 - cruise, VLM loads								
Objective	drag	0.001222	0.002621				1.00E+03	
Constraints	lift	0.142893	0.2	0.2			1.00E+01	
	stress	2.21477	1		0	1	1.00E+00	
Design Variables	camber	0			0	0.05	1.00E+02	
	twist	0			-10	10	1.00E-01	deg
	thickness	0.0035	0.00308		0.0025	0.0075	1.00E+03	m

Case 7 - 2.5g maneuver, VLM loads								
Objective	drag	0.001152	0.003084				1.00E+03	
Constraints	lift	0.133741	0.2	0.2			1.00E+01	
	stress	2.42559	1		0	1	1.00E+00	
Design Variables	camber	0			0	0.05	1.00E+02	
	twist	0			-10	10	1.00E-01	deg
	thickness	0.0035	0.00309		0.0025	0.0075	1.00E+03	m
Case 8 - angle of attack design variable, cruise, VLM loads								
Objective	drag	0.001222	0.002531				1.00E+03	
Constraints	lift	0.142893	0.2	0.2			1.00E+01	
	stress	2.21477	1		0	1	1.00E+00	
Design Variables	camber	0			0	0.05	1.00E+02	
	twist	0			-10	10	1.00E-01	deg
	thickness	0.0035	0.00303		0.0025	0.0075	1.00E+03	m
	angle of attack	2.5	0.0962		0	5	1.00E+00	deg
Aero-Structural								
	Name	**Baseline**	**Optimized**	**Target**	**Lower**	**Upper**	**Scaler**	**Units**
Case 9 - angle of attack design variable, 2.5g maneuver, VLM loads								
Objective	drag	0.001152	0.003014				1.00E+03	
Constraints	lift	0.133741	0.2	0.2			1.00E+01	
	stress	2.42559	1		0	1	1.00E+00	
Design Variables	camber	0			0	0.05	1.00E+02	
	twist	0			-10	10	1.00E-01	deg
	thickness	0.0035	0.00312		0.0025	0.0075	1.00E+03	m
	angle of attack	2.5	0.548		0	5	1.00E+00	deg
Case 10 - cruise, VLM loads								
Objective	mass	9632.998	7723.098				1.00E-03	kg
Constraints	lift	0.142893	0.2	0.2			1.00E+01	
	stress	2.21477	1		0	1	1.00E+00	
Design Variables	camber	0			0	0.05	1.00E+02	
	twist	0			-10	10	1.00E-01	deg
	thickness	0.0035	0.0025		0.0025	0.0075	1.00E+03	m
Case 11 - 2.5g maneuver, VLM loads								
Objective	mass	9632.998	7751.649				1.00E-03	kg
Constraints	lift	0.133741	0.2	0.2			1.00E+01	
	stress	2.42559	1		0	1	1.00E+00	
Design Variables	camber	0			0	0.05	1.00E+02	
	twist	0			-10	10	1.00E-01	deg
	thickness	0.0035	0.00251		0.0025	0.0075	1.00E+03	m

Appendix B: Software and Version Numbers

With many of the software packages and frameworks in the MBSA&E framework in active development, a list of software versions used are given for reference in the table below.

Software Package	Version
Aviary	0.9.3
Dymos	1.9.1
FUNtoFEM	0.3.7
MPhys	1.3.0
mpi4py	3.1.5
OpenAeroStruct	2.7.0
OpenMDAO	3.31.2
OpenVSP	3.31.1
pyCycle	4.2.1
pyGeo	1.13.1
pyOptSparse	2.10.2
SNOPT	7
TACS	3.6.0

References

1. Raymer, Daniel. *Aircraft design: a conceptual approach*. American Institute of Aeronautics and Astronautics, Inc., Ch. 20, p. 664, 1999.

2. Hange, Craig. "Performance Challenges of Hybrid Wing CESTOL Transports." *47th AIAA Aerospace Sciences Meeting including The New Horizons Forum and Aerospace Exposition*. 2009.

3. Bruner, Sam, et al. *NASA N+ 3 subsonic fixed wing silent efficient low-emissions commercial transport (SELECT) vehicle study*. No. NASA/CR-2010-216798/REVA. 2010.

4. Liebeck, Robert H. "Design of the blended wing body subsonic transport." *Journal of aircraft* 41.1 (2004): 10-25.

5. Hunsaker, Douglas F., and Warren Phillips. "Ludwig Prandtl's 1933 paper concerning wings for minimum induced drag, translation and commentary." *AIAA Scitech 2020 Forum*. 2020.

6. Reuther, James, et al. "A coupled aero-structural optimization method for complete aircraft configurations." *37th Aerospace sciences meeting and exhibit*. 1999.

7. Bowers, Albion H., et al. *On wings of the minimum induced drag: Spanload implications for aircraft and birds*. No. DFRC-E-DAA-TN19884. 2016.

8. Gray, Justin S., et al. "OpenMDAO: An open-source framework for multidisciplinary design, analysis, and optimization." *Structural and Multidisciplinary Optimization* 59 (2019): 1075-1104.

9. Wells, Douglas P., Bryce L. Horvath, and Linwood A. McCullers. *The flight optimization system weights estimation method*. No. NASA/TM-2017-219627/VOL1. 2017.